Optical Waveguide for Common Path Simultaneous Refractive Index and Broadband Absorption Measurements in Small Volumes

Gupta, Ruchi; Goddard, Nicholas J.

DOI:
10.1016/j.snb.2016.07.162

Document Version
Peer reviewed version

Citation for published version (Harvard):
Gupta, R & Goddard, NJ 2016, 'Optical Waveguide for Common Path Simultaneous Refractive Index and Broadband Absorption Measurements in Small Volumes', Sensors and Actuators B: Chemical, vol. 237, pp. 1066-1075. https://doi.org/10.1016/j.snb.2016.07.162

Optical Waveguide for Common Path Simultaneous Refractive Index and Broadband Absorption Measurements in Small Volumes

Corresponding author: Ruchi Gupta, Department of Chemistry, University of Hull, Cottingham Road, Hull, HU6 7RX, UK; Email: ruchi.gupta@hull.ac.uk; Phone: +44 148 246 6552.

Co-authors: Nicholas J. Goddard, Process Instruments (UK) Ltd, March Street, Burnley, BB12 0BT, UK; Email: nick.goddard1@outlook.com; Phone: +44 128 242 2835.

Abstract

Simultaneous refractive index monitoring and absorption spectroscopy in small volumes common to both measurements using single light source and detector are beneficial, but challenging to perform. This work presents an optical device consisting of a porous waveguide deposited on glass, which is called dye-doped leaky waveguide (DDLW), for this purpose. The waveguide was made of agarose doped with a dye, reactive blue 4. Glycerol and rhodamine 6G were used as an exemplar system to demonstrate the feasibility of DDLW to perform simultaneous refractive index and broadband absorption measurements in a small common volume of 3.5 nL. In this case, the immobilised reactive blue 4 permits visualisation of the resonance angle of the waveguide for refractive index monitoring, while the additional absorption caused by the free rhodamine 6G was determined by measuring the wavelength dependent additional losses in the reflectivity profile of the DDLW. The refractive index sensitivity and limit of detection of the DDLW was 106.32±0.97° RIU^{-1} and 2.82×10^{-6} respectively. By combining the two measurements, the DDLW was shown to be suitable to monitor the absorption spectrum and anomalous dispersion of rhodamine 6G as well as the nature of its interactions with reactive blue 4. These interactions resulted in enhancing the concentration of the rhodamine 6G in the waveguide by a factor between 119 and 191. The DDLW was shown to be suitable to obtain the absorption spectrum of rhodamine 6G at concentrations as low as 1 µM. Future work will focus on the application of the DDLW to characterise analytes/ determine parameters of biological significance such as iron loading per molecule of serum ferritin.

Keywords: Optical, porous, waveguide, absorption spectroscopy, refractive index.

1. Introduction

Label-free optical devices integrated with microfluidics are particularly suitable for high throughput screening of large number of biological samples available in small volumes [1-5]. Most current optical devices, however, do not permit simultaneous determination of refractive index and absorption changes. Interferometric devices such as Mach-Zehnder interferometers measure the phase difference between a sample and a reference beam by interfering the two and measuring changes in intensity as the phase difference caused by refractive index changes in the sample beam path changes [6]. Any change in intensity of the sample beam caused by absorption would also change the output intensity, thus making it difficult to deconvolute the two effects. Alternatively, interferometers rely on measuring fringe shifts to determine changes in refractive index. In order to probe a volume of sample, long coherence length light is required and hence a monochromatic light source is used to generate a fringe pattern as a function of angle of incidence [7]. In this case, fringe contrast is related to the absorption coefficient of the sample at the

wavelength of the monochromatic light source, thereby permitting absorption measurements in a narrow (50-100 nm), but not broad range of wavelengths [8]. Two light sources; a laser incident at oblique angle and white LED at normal incidence are used to perform simultaneous refractive index measurement and broadband absorption spectroscopy simultaneously on the same volume of sample [9]. The approach, however, has limitations. Firstly, the sensitivity and limit of detection (LOD) of absorption measurements using a spectrophotometer is limited because the optical pathlength is governed by the physical dimensions of the microfluidic channel [10]. Secondly, as LED light passes through the entire volume of the sample, it should be free of particles (e.g. cells) to avoid scattering. Thirdly, the use of two light sources and detectors makes the entire system bulkier and less integrated. In another report, a fabry-perot cavity was integrated with a microfluidic channel such that the two mirrors had ~60% reflectivity for ~1550 nm light [11]. As a result, light in the infrared region bounced between the mirrors and passed through the microchannel multiple times, thereby generating an interference pattern. The position of peaks and dips changed with refractive index of fluids in the microchannel. The mirrors were completely transparent to visible light, which was used to perform absorption spectroscopy. The approach, therefore, either required a source that can emit light in visible and infrared region or two sources. In addition, as light passed through the microchannel once only, the sensitivity and LOD were limited. Surface Plasmon Resonance (SPR) devices can determine both refractive index and absorption change by measuring the position and shape of the reflectivity dip [12], but the gold layer typically used makes it impossible to monitor changes at wavelengths below about 600 nm. Since the absorption maximum of many biological species (such as haemoglobin and serum ferritin) is below 600 nm, this makes SPR unsuitable for measurement of these species. Other metals such as aluminium can be used for SPR at shorter wavelengths, but the reactivity of metals other than gold means that such devices are relatively short-lived. Whispering gallery mode (WGM) resonators such as microspheres and ring resonators are widely used to measure changes in refractive index by monitoring extremely small shifts (typically pm) of narrow resonance linewidths (typically ~0.1 pm) [13-16]. Slightly non-spherical WGM are shown to be suitable to confine high order modes and consequently perform broadband absorption spectroscopy [17]. Simultaneous refractive index measurements and broadband absorption spectroscopy using these WGM resonators is, however, not shown. This may be because extremely small shifts introduced as a result of refractive index changes are difficult to measure for broad peaks, which is a characteristic of slightly non-spherical WGM resonators. Spectroscopic ellipsometry has been shown to be able to determine both absorption spectrum and refractive index of materials, but is typically used for thin films [18].

This work, for the first time, reports a device (called dye-doped leaky waveguide, DDLW) consisting of a dye-doped porous waveguide supporting a leaky optical mode, which was used for both refractive index measurements and broadband absorption spectroscopy. The presence of the dye immobilised in the waveguide permits visualising the resonance angle as a dip in the reflectivity curve. This approach of visualising the resonance angle permits using unpolarised light, tuning the dip parameters (e.g. depth) with ease, and fabricating these devices without requiring specialised equipment (e.g. sputtering of gold for SPR devices and e-beam evaporation to deposit titanium in case of metal-clad leaky waveguide, MCLW) [19]. While the shifts in the resonance angle position were related to changes in refractive index induced by a sample, the depth of the dip was a function of the wavelength-dependent absorbance of the sample. The dye concentration in the waveguide was optimised to produce a sharp dip for ease of refractive index monitoring,

while remaining shallow enough to provide a reasonable dynamic range for absorption measurements. Although MCLW and DDLW have similar sensitivity to refractive index change, the DDLW has a larger linear and dynamic range than the MCLW for absorption spectroscopy. The simpler fabrication and instrumentation required for the DDLW, along with the wider dynamic range for absorption spectroscopy and equal sensitivity to refractive index, indicate that the DDLW is preferred over the MCLW.

The DDLW developed in this work consists of an agarose waveguide spin coated on a glass slide and subsequently doped with reactive blue 4 (RB4). RB4 was chosen because it contains a dichlorotriazine group, which reacts with hydroxy groups in agarose under basic conditions. RB4 also has a broad absorption that allows the resonance angle to be determined over most of the visible region. The refractive index sensitivity of the DDLW developed in this work was determined by using solutions containing different concentrations of glycerol. In contrast to conventional high index waveguides, which rely on the interaction of light in the evanescent field with the sample, the sensitivity of porous waveguides to changes in bulk refractive index was largely independent of waveguide thickness. This is because the sample can diffuse into porous waveguides and hence all of the light (i.e. present in the waveguide and evanescent field) interacts with the sample. The suitability of DDLW to perform broadband absorption spectroscopy was demonstrated by using rhodamine 6G, which has an absorption spectrum that overlaps with reactive blue 4, as an exemplar analyte. The absorption measurements performed using the DDLW also showed that there is a reversible (possibly, electrostatic) interaction between rhodamine 6G and reactive blue 4. Finally, rhodamine 6G was added to glycerol solutions, and its absorption spectrum as well as changes in refractive index in the vicinity of the waveguide introduced as a result of anomalous dispersion and sample composition were studied simultaneously.

2. Experimental

1 mm thick glass slides were purchased from VWR (Leicestershire, UK). Ultrapure™ LMP agarose was obtained from Life Technologies (Paisley, UK). Glutaraldehyde (25%), sodium hydroxide, potassium chloride, reactive blue 4 (35%), phosphate buffered saline (PBS, 20 mM, pH 7.4), rhodamine 6G (R6G) and glycerol were purchased from Sigma-Aldrich (Gillingham, UK).

2.2 DDLW device fabrication

Glass slides were cut into squares of ~25.4 mm by 25.4 mm using a diamond scribe, and cleaned in an ultrasonic bath with soap solution, de-ionised water and ethanol for 30 min each. In order to investigate the effect of the concentration of agarose solution used to make the waveguide, either 0.1, 0.2 or 0.3 g of agarose was added to 10 ml of de-ionised of water. The solution was heated in a microwave oven until the agarose was fully dissolved, following which it was placed on a hot plate set at 95 °C. 12.5 µl of 25% (v:v) glutaraldehyde was then added and allowed to react for 15 min. Subsequently, the solution was spin coated at 2250 rpm for 30 s. Reactive blue 4 was immobilised in the agarose layer by immersing it in a solution containing 0.78 mM of the dye, 0.268 M KCl and 10 mM NaOH. The reaction time between RB4 and agarose was monitored by recording the dip in real-time to determine the optimum reaction time. The plate used to make a flow cell consisted of a 0.2 mm deep and 4 mm wide cavity, a groove to mount an O-ring, and an inlet and outlet. The flow cell was placed on the agarose coated glass and held in place using a fixture.

2.3 Instrumentation

The experimental set-up used in this work is shown in Figure 1. Briefly a BK7 equilateral prism of 30 mm by 30 mm (Qioptic Photonics, Denbighshire, UK) was used to couple light in and out of DDLW. A tungsten-halogen lamp (Ocean Optics, Duiven, Netherlands) and CMOS camera (PL-B781, Pixelink, Ottowa, Canada) were mounted on rails, which were connected to goniometers to control their angular position. The light source and camera were located ~150 mm and ~120 mm away from the prism respectively. Thus, the overall dimension of the set-up was ~250 mm × 80 mm × 30 mm placed in a light-tight box of external dimensions 600 mm × 600 mm × 350 mm.

Light was passed through an assembly of achromatic doublet and cylindrical lens to obtain a wedge-shaped beam, which permit illuminating the DDLW with a range of angles of incidence simultaneously. The beam width at the waveguide was 0.5 mm. The focal length of the cylindrical lens used was 100 mm, which resulted in light of wedge angle of ~14° in air or ~9° in the prism. The output of the DDLW was passed through a transmission grating (Thorlabs GT25-03, 300 lines mm^{-1}, blaze angle 17.5°) to disperse the output light and then an achromatic doublet (Comar Optics 100 DQ 25) to focus it onto the camera. The camera integration time was 7 ms. The relationship between camera pixel and wavelength was determined by introducing interference filters of known wavelength in the path of incident light and recording the corresponding position of reflected light on the camera. Refractive indices of solutions ($n_{D,20}$) were determined using a Bellingham and Stanley RFM900 refractometer. Fluids were pumped through the flow cell using a peristaltic pump at a flow rate of 0.2 ml min^{-1}. Conventional absorption spectra were obtained using the tungsten-halogen source, a 1 cm path length cuvette and a fibre-coupled spectrophotometer (USB4000, Ocean Optics, Duiven, Netherlands).

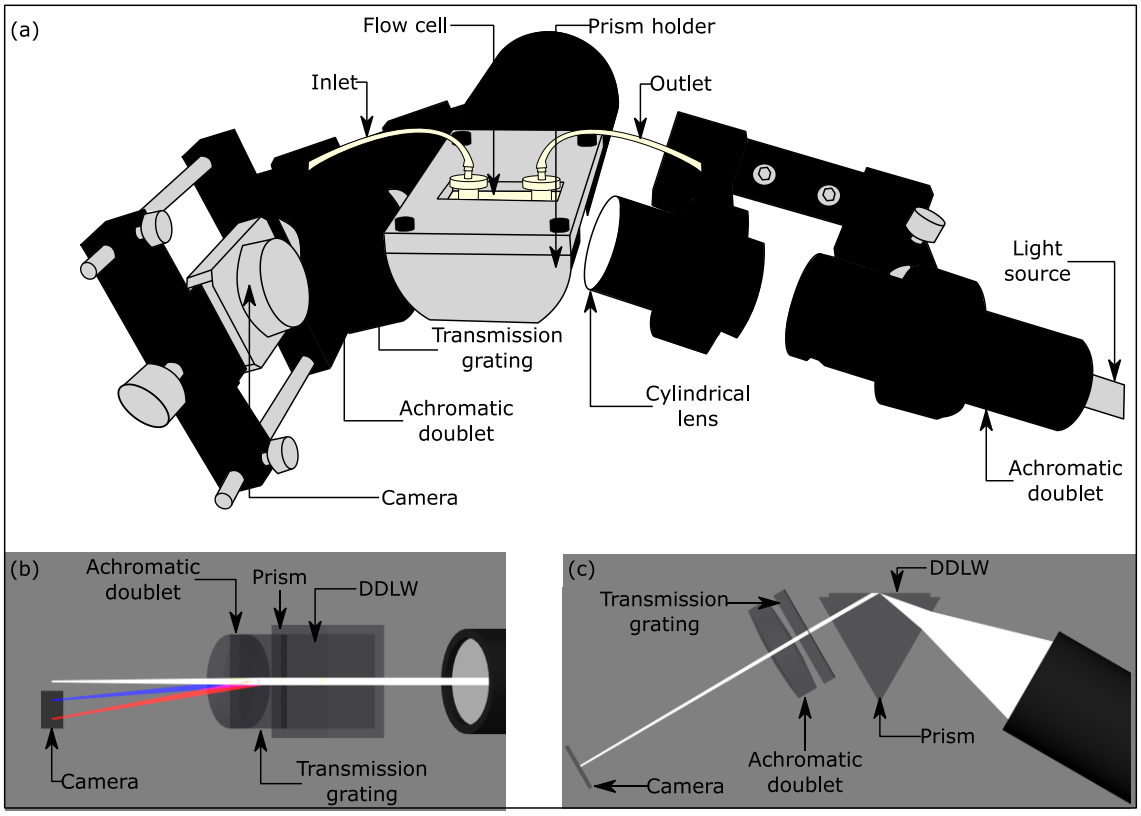

Figure 1: Schematic of the set-up used to test the DDLW device, (b) plan and (c) side views of the arrangement (where the flow cell is not shown in (b) and (c) for clarity)

3. Results and discussion

3.1 Modelling

Modelling of the devices was carried out using an in-house transfer matrix program written in C++. The program contains a database of materials and uses either cubic spline interpolation or polynomial evaluation to generate complex refractive indices at different wavelengths. The imaginary refractive index of the dyes was generated from absorbance data obtained from known concentrations of the dye in a 1 cm cuvette in an Ocean Optics USB4000 spectrophotometer using the relationship:

$$K = \frac{100(\ln 10)\lambda\varepsilon c}{4\pi} \tag{1}$$

Where K is the (Napierian) imaginary refractive index, λ is the wavelength (m), ε is the (decadic) extinction coefficient of the dye (M^{-1} m^{-1}) at λ and c is the dye concentration (M). The factor of 100 was a result of converting the units of extinction coefficient of the dye from M^{-1} cm^{-1} to M^{-1} m^{-1}. The modelling program contains a recursive descent expression evaluator which allows the user to vary the optical structure parameters in a simple fashion by using named materials (such as NBK7, Ti, H_2O, Agarose_re and RB4) in any of the device layers. The dye's imaginary refractive index was calculated for a concentration of 1 µM, and can be varied simply by multiplying by an appropriate scaling factor. Figure 2 (a) and (b) shows the theoretical reflectivity curves of the DDLW and MCLW respectively with the same waveguide layer (1.53 µm agarose of refractive index of 1.35603) in response to different concentrations of RB4 in the waveguide layer.

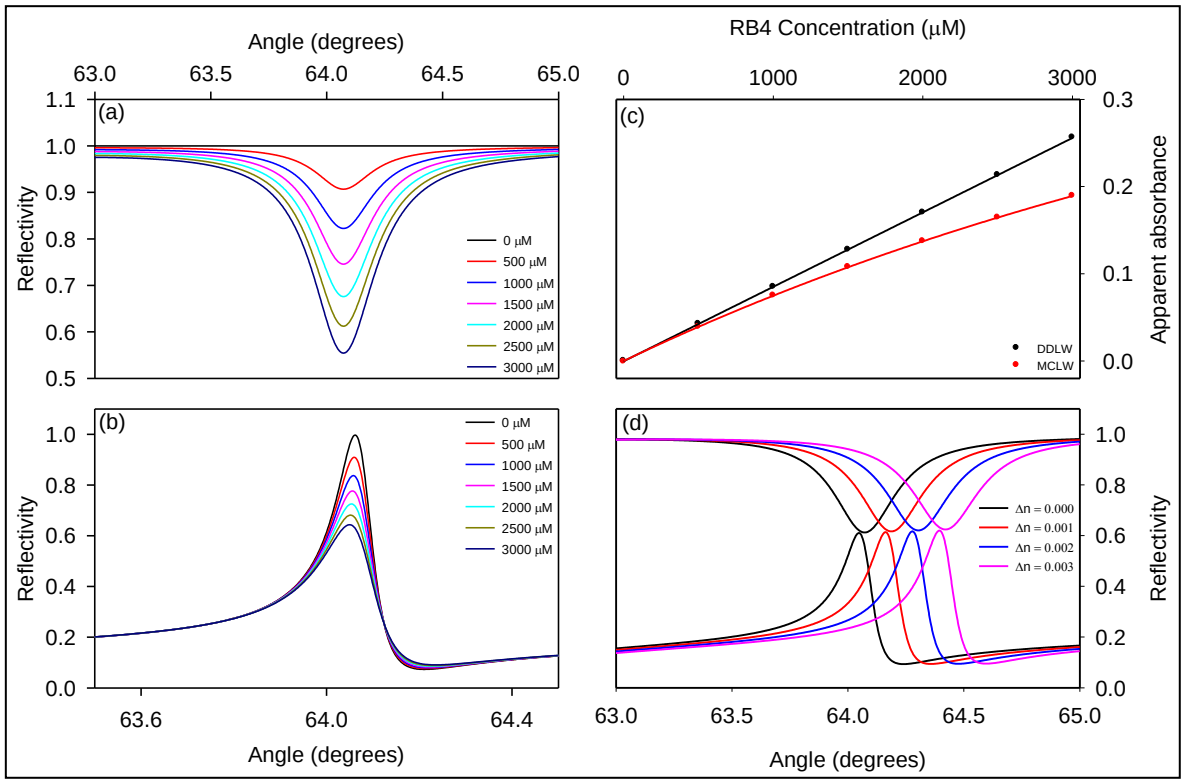

Figure 2: Theoretical reflectivity curves of a (a) DDLW and (b) MCLW with different concentrations of RB4 in the waveguide layer, (c) theoretical apparent absorbance and (d) refractive index sensitivity

In the case of a cuvette-based absorption measurement, absorbance is related to the transmittance, which is the ratio of the intensity of transmitted and incident light. In the case of the waveguide, the transmitted light is represented by the light that couples out of the waveguide, so the reflectivity in the case of the waveguide is equivalent to the transmittance of a cuvette. The theoretical apparent absorbance was calculated from this data using a modified Beer-Lambert equation:

$$A = log\left(\frac{R_0}{R}\right) \tag{2}$$

Where A is the apparent absorbance, R_0 is the reflectivity at zero concentration at the peak or dip position and R is the minimum reflectivity of the dip (for DDLW) or maximum reflectivity of the peak (for MCLW) at a given RB4 concentration. Figure 2 (c) shows how the theoretical apparent absorbance changes with RB4 concentration in the waveguide layer for both types of devices. The response of MCLW to RB4 concentration is non-linear, while that of DDLW mode is substantially linear over a large concentration range of the dye. At low concentrations the MCLW is almost as sensitive as the DDLW, but at higher concentrations its sensitivity drops, reducing the available dynamic range. Figure 2 (d) shows the theoretical dip and peak shifts for waveguide refractive index increments of 0, 0.001, 0.002 and 0.003 for DDLW and MCLW respectively. This in turn illustrates that the refractive index sensitivity of both devices was almost identical. Modelling (not shown) also indicates that the sensitivity to real refractive index change in the waveguide is independent of the concentration of RB4.

3.2 Preliminary results

Figure 3 (a) shows a typical one dimensional reflectivity profile of devices consisting of a waveguide made of 1%, 2% and 3% (all: w:v) agarose solutions spin coated at 2250 rpm and incubated for 120 min in RB4 solution. The resonance angle appears as a dip in the reflectivity curve because light travelling in the dye-doped waveguide is absorbed. Based on Figure 3, a waveguide made of 1% (w:v) agarose solution did not support an optical mode at 589 nm because it was too thin. While the waveguide made of 2% (w:v) solution supported one optical mode, the waveguide made of 3% (w;v) agarose solution was thick enough to support three optical modes. The remaining work was performed using the single-moded DDLW with a waveguide made of 2% (w:v) agarose solution where the dip position and depth were used for refractive index and broadband absorption measurements respectively.

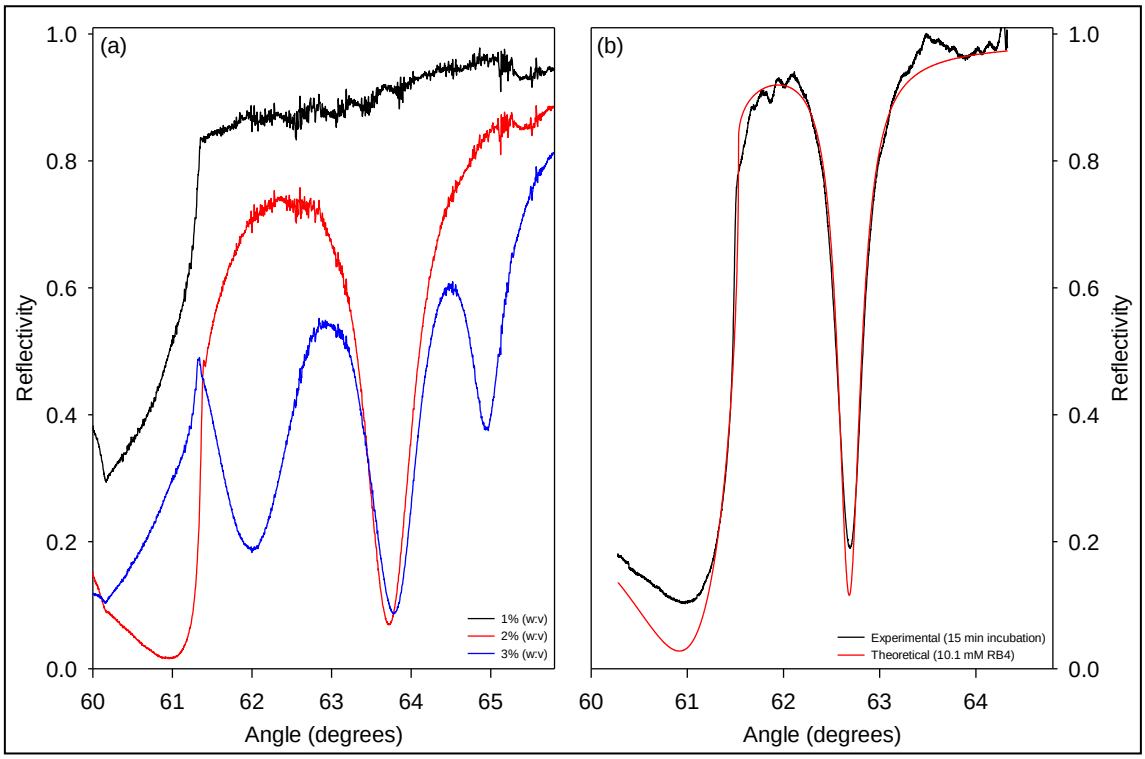

Figure 3: Output profile of DDLW at 589 nm for different (a) concentrations of agarose solution (where DDLWs were incubated in RB4 for 120 min) and (b) comparison of experimental and theoretical output of DDLW

Further, the amount of RB4 immobilised in the agarose waveguide depends on the time for which the DDLW was incubated in the dye solution. The incubation time of the device in RB4 solution had a significant influence on the shape and depth of the dip because it affects the concentration of the dye immobilised in the waveguide. For incubation times shorter than 15 min, the concentration of RB4 immobilised in the waveguide was small. As a result, the dip in the reflectivity was shallow resulting in difficulties in monitoring its position. For incubation times higher than 15 min, the depth of the dip initially increased following which, the dip became broad and shallow. The dynamic range of absorption spectroscopy decreases as the depth of the dip increases, so 15 min incubation was, therefore, determined to be optimum because it resulted in a sharp dip permitting facile tracking of the angular position for refractive index sensing, whilst preserving a reasonable dynamic range for absorption monitoring.

The typical output of a DDLW consisting of agarose waveguide incubated in RB4 for 15 min is shown in Figure 3 (b). The imaginary refractive index of RB4 doped waveguides of given thickness and real refractive index depends on the wavelength dependent extinction coefficient and concentration of the dye immobilised in the waveguide, and affects the depth of the dip. While the wavelength dependent extinction coefficient of RB4 was determined using the Ocean Optics USB4000 spectrophotometer, the transfer matrix program was used to estimate the concentration of the dye immobilised in the waveguide. Modelling was also used to estimate the thickness and swelling ratio (S, the ratio of the volume of the rehydrated gel to that of an undehydrated gel), which affects the real refractive index of the waveguide. The real refractive index of rehydrated (n_R) agarose at each wavelength is given by the following expression:

$$n_R = n_W + \frac{c\Delta n}{S} \quad (3)$$

Where c is the concentration of the original agarose solution (w:v), n_W is the refractive index of water and Δn is the refractive index increment for pure agarose with respect to water. For example, the refractive index of a rehydrated agarose with a swelling ratio of 13.5% is 1.35603 (*versus* 1.33641 for undehydrated gel) at 589 nm. Measuring these parameters for a low concentration wet gel is, however, challenging using conventional techniques. To estimate the swelling ratio, thickness and RB4 concentration in the waveguide, the device that had been reacted with RB4 was subsequently irrigated with PBS until no further change in the output of the device was visible. An image of the device output was then taken, the dark image was subtracted and the resulting background corrected image was normalised by division by a background corrected image taken using a plain glass slide. A profile in angle was then extracted centred at 589 nm using ImageJ and the resulting reflectivity profile imported into the transfer matrix program. A simplex optimisation routine then provided the best fit values for the waveguide thickness, swelling ratio and RB4 concentration. The best fit to the experimental data shown in Figure 3 (b) was found with a swelling ratio (S) of 13.5% (agarose concentration 14.8%), thickness of 1.53 µm and RB4 concentration of 10.1 mM. This means that the original gel, containing 2% w/v agarose was dried down and then, when rehydrated, swelled up to 14.8% w/v agarose resulting in a thinner, higher refractive index waveguide than the original deposited film. With a flowcell width of 4 mm, a beam width of 0.5 mm and a sensing depth (the waveguide thickness plus the penetration depth of the evanescent field) of 1.767 µm, the volume interrogated is only 3.5 nL.

3.3 Refractive index measurements using DDLW

A typical two dimensional output of a DDLW consisting of a waveguide made of 2% (w:v) agarose solution and incubated in RB4 for 15 min is shown in Figure 4 (a). The positions corresponding to the total internal reflection (TIR) and resonance angle are also marked in Figure 4 (a). Figure 4 (a) shows that the position of the resonance angle decreases as the wavelength increases. Solutions of different concentrations of glycerol were introduced for 600 s, and images obtained at the end of this period were analysed to obtain the wavelength dependent dip position. The resulting plot is shown in Figure 4 (b), which shows that the resonance angle decreases by ~0.60° as the wavelength increases from 430 nm to 675 nm. The relationship between the shift in dip position ($\Delta\theta_R$) of the zero-order mode and refractive index of glycerol solutions ($n_{D,20}$) at 589 nm is given by $\Delta\theta_R = 106.32 n_{D,20} - 141.76$ (r^2:0.999, shown in Figure 4 (c)). Thus, the refractive index sensitivity of the DDLW is 106.32±0.97° RIU^{-1}, which is comparable to the theoretical sensitivity (108.68° RIU^{-1}). The refractive index limit of detection, based on the refractive index sensitivity to glycerol and the three times the standard deviation of the angular position of the dip (1.00×10^{-4} °), is 2.82×10^{-6}. The refractive index sensitivity of a 1.53 µm porous waveguide of refractive index of 1.35603 is ~10 times higher than the refractive index sensitivity of a non-porous waveguide of the same thickness and refractive index (results not shown). The refractive index sensitivity of the porous waveguide is largely independent of its thickness because the sample can diffuse into porous waveguides and hence all of the light (i.e. present in the waveguide and evanescent field) interacts with the sample. This is in contrast to a non-porous waveguide where only the evanescent field interacts with the sample. The fraction of light in the evanescent field and hence the refractive index sensitivity decreases as the thickness of a non-porous waveguide increases. In addition, the refractive index sensitivity of a porous waveguide is largely independent of wavelength, but reduces as the wavelength decreases for a non-porous waveguide. To validate the waveguide model, the

experimental reflectivity profiles at 589 nm were fitted using the (fixed) previously determined model parameters but with the addition of a (variable) refractive index increment (Δn_{inc}) in both the waveguide and cover layers. Figure 4 (d) shows a plot of the fitted refractive index increment against the refractive index of the glycerol concentration (n_{gly}). The slope of the line was 0.985 (r^2:0.999), which indicates that the model fitted well with the experimental data.

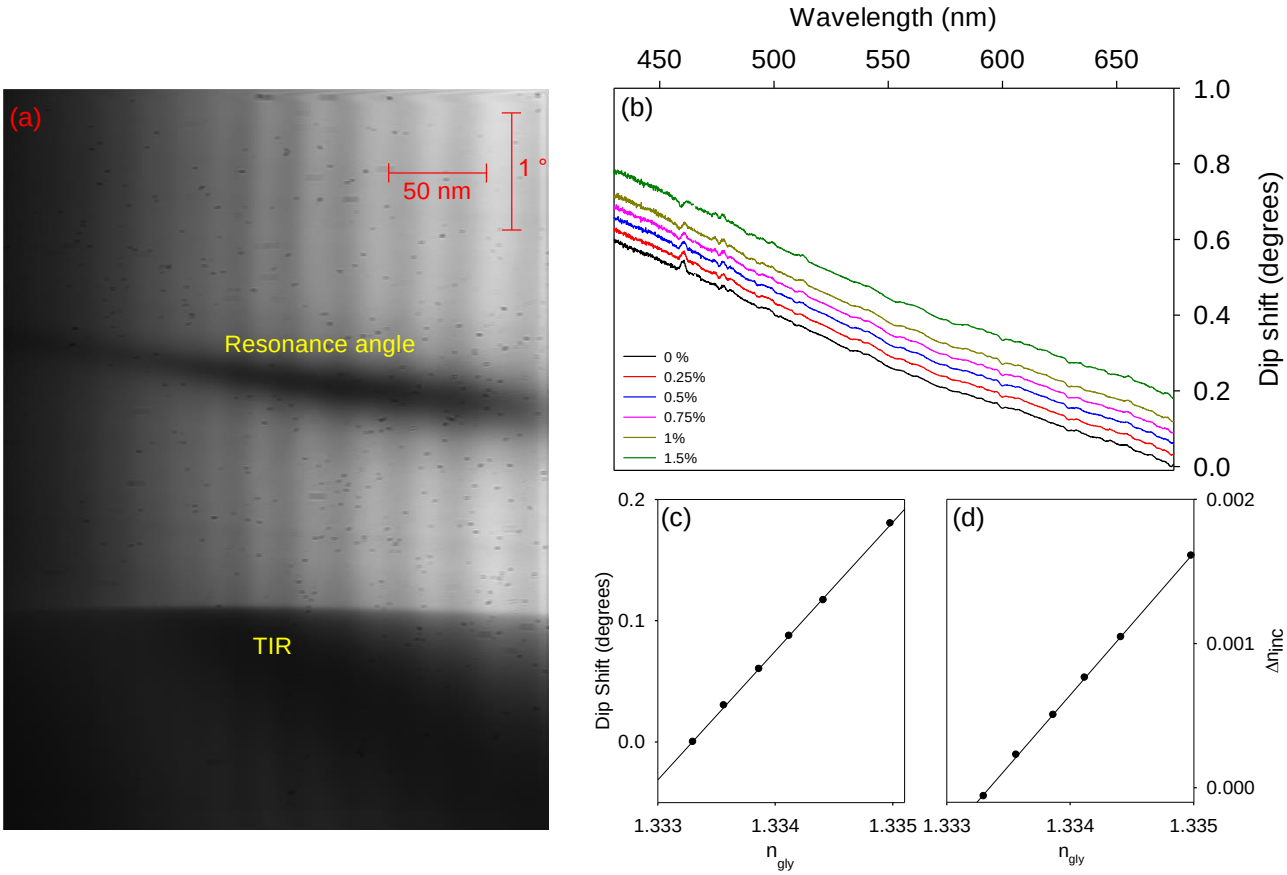

Figure 4: (a) Typical output profile of DDLW irrigated with PBS, (b) wavelength dependent dip position, (c) dip position and (d) theoretical refractive index increment of waveguide *versus* refractive index of glycerol respectively at 589 nm

R6G solutions from low to high concentration were introduced on top of DDLW consecutively and allowed to equilibrate for 1000 s following which the output of the DDLW was captured. Figure 5 (a) shows the output of the RB4 doped DDLW devices after being irrigated with 12.5 µM R6G solution for 1000 s, which shows that the presence of R6G in the waveguide gives rise to anomalous dispersion near the absorption maximum of the dye, leading to an increase in dip position with increasing wavelength in the range 490 nm to 540 nm. A plot of corresponding shifts in the dip position of the DDLW as a function of wavelength for different concentrations of R6G solutions is provided in Figure 5 (b). As shown in Figure 5 (b), the anomalous dispersion increases as the concentration of R6G solution increases.

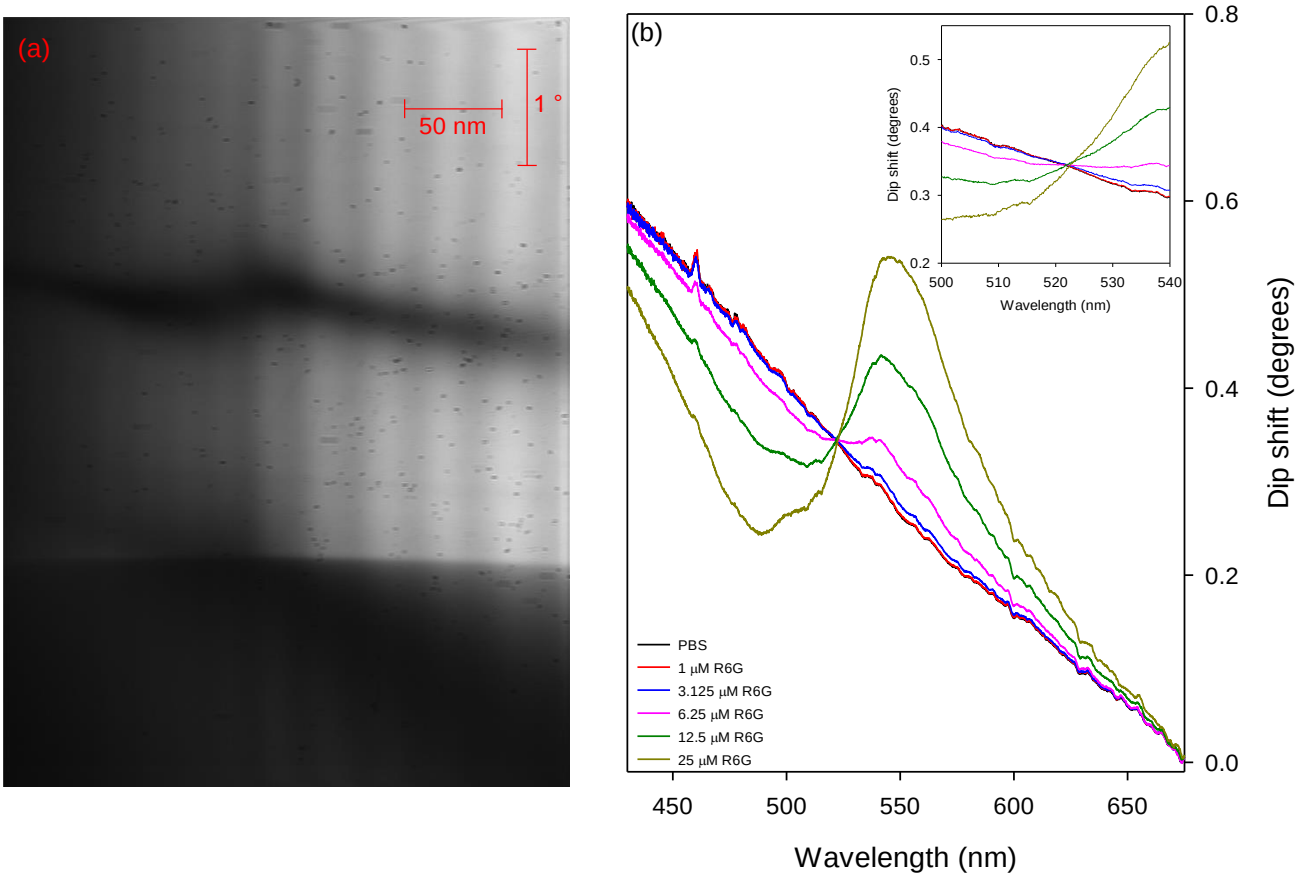

Figure 5: (a) Output of the RB4 doped DDLW with 12.5 µM R6G and (b) change in dip position as a function of wavelength at different R6G concentrations

3.4 Absorption spectroscopy using DDLW

Absorption spectra of R6G obtained using the Ocean Optics USB4000 spectrophotometer at different concentrations of the dye are shown in Figure 6 (a). As shown in Figure 6 (a), R6G absorbs between 435 nm and 570 nm with absorption maxima at 527-531 nm and 498-500 nm for monomeric and dimeric forms respectively. This is consistent with literature reported values [20]. Figure 6 (a) also shows that R6G begins to form dimers at concentrations as low as 6.25 µM in PBS, which is accordance with literature [21]. Further, a comparison of absorption spectra of 12.5 µM R6G in PBS and 37.5 µM RB4 solution shows that the spectrum of R6G was red shifted by ~5 nm in the latter case indicating that the two dyes interact. In addition, in the latter case, the absorbance between 570 nm and 675 nm was less than zero, suggesting that the absorption of RB4 decreases as a result of its interaction with R6G. The relationship between the peak absorbance (A_{peak}) *versus* the concentration of R6G solution ([R6G]) (see Figure 6 (a)) is linear in the selected concentration range of the dye. The relationship between the two is given by the following expression: $A_{peak}=0.026+0.062\times[R6G]$ (r^2: 0.997). The absorption spectra of 12.5 µM R6G prepared in different concentrations of glycerol solutions were also acquired, and were similar to the spectrum of the same concentration of the dye in PBS (results not shown).

The DDLW was consecutively irrigated with PBS and different concentrations of R6G (from low to high) each for 1000 s and the corresponding output was captured. The gray scale value corresponding to the resonance dip of the DDLW was found for each wavelength and substituted in Equation 2 to obtain the absorbance spectra of different concentrations R6G (shown in Figure 6 (b)). The absorption spectra of 1 µM and 3.125

µM of R6G including the wavelength corresponding to the absorbance peak, obtained using DDLW is similar to that recorded *via* the Ocean Optics USB4000 spectrophotometer. As DDLW is flushed with increasing concentrations of R6G, the absorbance peak at ~490 nm increases whereas that at ~530 nm decreases, thereby suggesting the formation of either higher aggregates of R6G on/ in the hydrogel [22] or the formation of R6G-RB4 complexes. In addition, as the concentration of R6G increases, the absorbance peak corresponding to the monomeric form of the dye was red shifted. Further, based on negative absorbance values from 570 nm to 675 nm, the absorbance of RB4 decreases as the concentration of R6G increases. These changes in the absorption spectra of RB4 and R6G indicate that the two dyes interact strongly with each other.

Figure 6: (a) Absorbance spectrum of R6G obtained using (a) Ocean Optics USB4000 spectrophotometer **(where the inset shows peak absorbance *versus* the concentration of R6G) and (b) DDLW (where inset (i) illustrates the output of device with undoped agarose waveguide flushed with 1 mM R6G and inset (ii) shows the corresponding absorption spectrum)**

1mM R6G was introduced on top of a device consisting of an updoped agarose waveguide. The resulting output and the absorption spectrum for this case are shown in insets in Figure 6 (b). A comparison of absorption spectra of R6G obtained using device consisting of agarose waveguides without and with immobilised RB4 suggests that the concentration of R6G in the agarose waveguide was higher than in the bulk in the latter case. This observation further supports the hypothesis that there is a strong interaction between RB4 and R6G. The enhancement factor (i.e. the ratio of the concentration of R6G in the waveguide and bulk) is estimated to be between 119 and 191 depending on the bulk R6G concentration. Subsequently, the DDLW was flushed with PBS, and the wavelength dependent dip position and depth returned back to their original values. This implies that there is a reversible interaction between R6G and RB4. It is likely that the interaction between the two dyes is electrostatic because while R6G is a cationic dye, RB4 is anionic as a result of the presence of sulfonate groups.

3.5 Simultaneous refractive index and broadband absorption measurements using DDLW

Subsequently, the DDLW was irrigated with 6.25 µM R6G prepared in PBS until no further change in the position of the dip was observed. Subsequently, solutions of 6.25 µM R6G prepared in different concentrations of glycerol were introduced onto the DDLW, and the corresponding outputs were recorded. A plot of change in the position of the dip against time is shown in Figure 7 (a). The relationship between the shift in dip position ($\Delta\theta_R$) and the refractive index of glycerol solutions ($n_{D,20}$) at 589 nm is given by $\Delta\theta_R = 104.70 n_{D,20} - 139.70$ (r^2: 0.998). Thus, the refractive index sensitivity of DDLW for glycerol solutions consisting of 6.25 µM of R6G is 104.70±2.28° RIU^{-1}. A comparison of the plots of the shift in dip position *versus* the refractive index of glycerol solutions without and with R6G (Figure 7(a) inset (i)) shows that the refractive index sensitivity values of DDLW in the two cases are comparable. Figure 7(a) inset (ii) shows that the presence of anomalous dispersion does not affect the refractive index sensitivity of the DDLW. Figure 7(b) shows the absorption spectra of 6.25 µM R6G in different glycerol concentrations. These show that the spectra are similar in shape and peak wavelength, but show a trend towards increasing absorbance with increasing glycerol concentration. The glycerol solutions were pumped sequentially from low to high concentration. The increasing trend in absorption of R6G with glycerol concentration, which was not

observed in spectra obtained using the Ocean Optics USB4000 spectrophotometer, is likely to be a result of continuing binding of the dye to immobilised RB4 as each solution was pumped through the flowcell. Nevertheless, this work shows that it is possible simultaneously to monitor both broadband absorbance and refractive index using the DDLW. Like any absorption spectrophotometric technique, calibration is required to determine extinction coefficients of species which can then be used to find their concentration in samples of unknown composition.

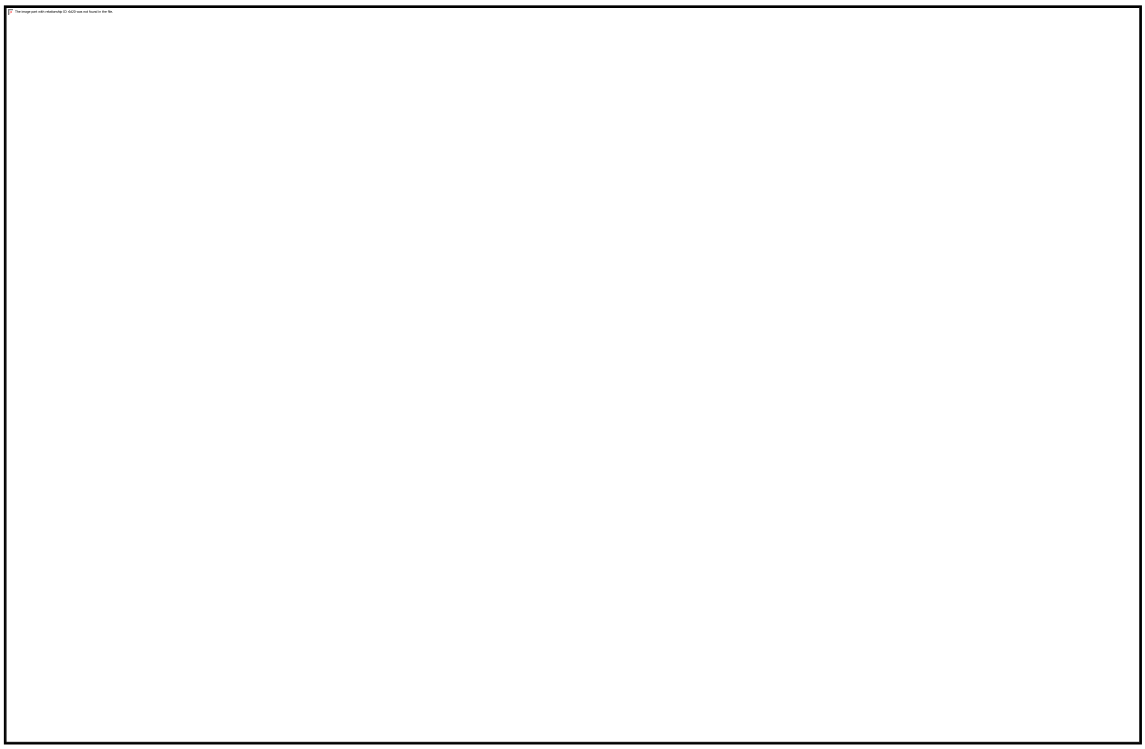

Figure 7: (a) Plot of dip position as a function of time for different glycerol solutions containing 6.25 μM R6G (where inset (i) shows the linear relationship between dip position and refractive index for glycerol solutions without and with R6G, inset (ii) shows the wavelength dependent dip position for glycerol with R6G) and (b) the absorption spectra of 6.25 μM R6G in different glycerol concentrations

4. Conclusions

By using an unpolarised white light source to illuminate a DDLW, followed by a transmission grating to disperse the light emerging from the device, it has been possible to perform simultaneous broadband absorption spectroscopy and refractive index monitoring in a common small volume. Previous techniques used for this purpose have either required separate instrumentation for the two parameters or have not been able to perform broadband measurements. The DDLW device is also very simple to fabricate, consisting of a spin-coated dyed agarose gel layer on a microscope slide. Unlike SPR, DDLW does not require an expensive high index substrate and can work over a much wider range of wavelengths. The concentration of agarose solution and spin speed used to fabricate the waveguide was optimised to obtain a DDLW that can support a single optical mode. The evolution of the reflectivity dip, which was observed at the resonance angle, caused by the reaction of the RB4 with agarose was monitored in real time. This was done to ensure that the dip was sharp so that its position could be easily determined for refractive index monitoring and not so deep that the dynamic range for absorption measurement would be compromised. It was found that 15 min incubation with 0.78 mM RB4 in 0.268 M KCl and 10 mM NaOH gave a dip suitable for both

measurements. Modelling using the transfer matrix method was used to estimate the waveguide thickness, swelling ratio and concentration of immobilised RB4 (1.53 µm, 13.5% and 10.1 mM respectively). The suitability of the DDLW for both absorption and refractive index monitoring was investigated using a combination of R6G and glycerol solutions. The refractive index sensitivity at 589 nm of the DDLW was found for glycerol solutions without and with R6G and were found to be comparable (106.32±0.97 and 104.70±2.28° RIU^{-1} respectively). In addition, the DDLW was shown to be suitable for absorption spectroscopy and refractive index monitoring over the wavelength range 430 - 675 nm, limited by the tungsten-halogen light source and the transmission grating. Refractive index monitoring over the entire wavelength range showed strong anomalous dispersion between 490 and 534 nm when R6G was introduced into the DDLW. Concentrations of R6G as low as 1 µM were observed to give significant absorption when the agarose waveguide was doped with RB4, but not when the waveguide was undoped. Since R6G is cationic and RB4 anionic, it is likely that there is a strong electrostatic interaction between the two dyes that enhances the local concentration of R6G when RB4 is present, resulting in concentration enhancement factors as high as 191. The dimerisation of R6G and/or its interaction with RB4 induced changes in the spectra of both dyes, increasing the shoulder at 490 nm for R6G and decreasing the extinction coefficient of RB4 between 570 and 675 nm. This work has shown that it is possible to perform broadband absorption spectroscopy in parallel with refractive index monitoring in small volumes. With a detection volume of only 3.5 nL, it is possible to detect sub-pmol amounts of R6G without concentration enhancement and fmol amounts with concentration enhancement using RB4 as a binding partner.

Future work will focus on the application of DDLW to estimate iron loading per molecule of ferritin where antibodies against serum ferritin will be immobilised in the agarose waveguide. Subsequently, refractive index measurements and broadband absorption spectroscopy will be performed to determine the concentration of serum ferritin and bound iron respectively. This is important because of an increasing body of evidence that suggests that serum ferritin and its iron loading plays a significant role in neurodegenerative disorders such as Alzheimer's Disease. Future work will also focus on immobilising a suitable combination of dyes in the agarose waveguide and exploiting their anomalous dispersion to devise a DDLW sensor that is insensitive to wavelength changes because of temperature effects over the entire visible region.

References

[1] S. Choi, M. Goryll, L.Y.M. Sin, P.K. Wong, J. Chae, **Microfluidic-based biosensors toward point-of-care detection of nucleic acids and proteins**, Microfluid. Nanofluid., 10, (2011), 231-247.

[2] H. Lee, L. Xu, D. Koh, N. Nyayapathi, K.W. Oh, **Various on-chip sensors with microfluidics for biological applications**, Sensors, 14, (2014), 17008-17036.

[3] B.E. Rapp, F.J. Gruhl, K. Laenge, **Biosensors with label-free detection designed for diagnostic applications**, Anal. Bioanal. Chem., 398, (2010), 2403-2412.

[4] S.-T. Yang, X. Zhang, Y. Wen, **Microbioreactors for high-throughput cytotoxicity assays**, Curr. Opin. Drug Discovery Dev., 11, (2008), 111-127.

[5] G. Luka, A. Ahmadi, H. Najjaran, E. Alocilja, M. DeRosa, K. Wolthers, A. Malki, H. Aziz, A. Althani, M. Hoorfar, **Microfluidics integrated biosensors: a leading technology towards lab-on-a-chip and sensing applications**, Sensors, 15, (2015), 30011-30031.

[6] E. Makarona, P. Petrou, S. Kakabakos, K. Misiakos, I. Raptis, **Point-of-Need bioanalytics based on planar optical interferometry**, Biotechnol. Adv., 34, (2016), 209-233.

[7] G. Gauglitz, **Direct optical sensors: principles and selected applications** Anal. Bioanal. Chem., 381, (2005), 141-155.

[8] M. Malak, F. Marty, T. Bourouina, D. Angelescu, **Simultaneous measurement of liquid absorbance and refractive index using a compact optofluidic probe**, Lab on a Chip, 13, (2013), 2682-2685.

[9] L.E. Helseth, **Simultaneous measurements of absorption spectrum and refractive index in a microfluidic system**, Opt. Exp., 20, (2012), 4653-4662.

[10] H. Gai, Y. Li, E.S. Yeung, in B.C. Lin (Editor), Microfluidics: Technologies and Applications, 2011, p. 171-201.

[11] J.B. Tillak, I. Bernacka-Wojcik, D. Barata, P.A.S. Jorge, H. Aguas, A.G. Oliva, in M.F.M. Costa (Editor), Int. Conf. App. Opt. Photon., 2011.

[12] X. Guo, **Surface plasmon resonance based biosensor technique: A review**, J. Biophotonics, 5, (2012), 483-501.

[13] C. Ciminelli, C.M. Campanella, F. Dell'Olio, C.E. Campanella, M.N. Armenise, **Label-free optical resonant sensors for biochemical applications**, Prog. Quant. Electron., 37, (2013), 51-107.

[14] L. He, S.K. Oezdemir, L. Yang, **Whispering gallery microcavity lasers**, Laser Photon. Rev., 7, (2013), 60-82.

[15] V.S. Ilchenko, A.B. Matsko, **Optical resonators with whispering-gallery modes - Part II: Applications**, IEEE J. Sel. Top. Quantum Electron., 12, (2006), 15-32.

[16] A.N. Oraevsky, **Whispering-gallery waves**, Quantum Electron., 32, (2002), 377-400.

[17] S.L. Westcott, J. Zhang, R.K. Shelton, N.M.K. Bruce, S. Gupta, S.L. Keen, J.W. Tillman, L.B. Wald, B.N. Strecker, A.T. Rosenberger, R.R. Davidson, W. Chen, K.G. Donovan, J.V. Hryniewicz, **Broadband optical absorbance spectroscopy using a whispering gallery mode microsphere resonator**, Review of Scientific Instruments, 79, (2008).

[18] V. Schmiedova, P. Heinrichova, O. Zmeskal, M. Weiter, **Characterization of polymeric thin films for photovoltaic applications by spectroscopic ellipsometry**, Applied Surface Science, 349, (2015), 582-588.

[19] R. Gupta, B. Bastani, N.J. Goddard, B. Grieve, **Absorption spectroscopy in microfluidic flow cells using a metal clad leaky waveguide device with a porous gel waveguide layer**, Analyst, 138, (2013), 307-314.

[20] D. Toptygin, B.Z. Packard, L. Brand, **Resolution of absorption spectra of rhodamine 6G aggregates in aqueous solution using the law of mass action**, Chem. Phys. Lett., 277, (1997), 430-435.

[21] R. Vogel, M. Harvey, G. Edwards, P. Meredith, N. KHeckenberg, M. Trau, H. Rubinsztein-Dunlop, **Dimer-to-monomer transformation of rhodamine 6G in aqueous PEO-PPO-PEO block copolymer solutions**, Macromol., 35, (2002), 2063-2070.

[22] M.J.T. Estevez, F.L. Arbeloa, T.L. Arbeloa, I.L. Arbeloa, R.A. Schoonheydt, **Spectroscopy study of the adsorption of rhodamine-6G on laponite-B for low loadings**, Clay Minerals, 29, (1994), 105-113.